Energy Spectrum of Milagro Sources

Andrew J. Smith* for the Milagro collaboration
**University of Maryland, College Park, MD 20742 USA*

Abstract. **The Milagro Gamma-Ray Observatory has detected numerous sources of VHE gamma-rays with a median energy above 20 TeV. The large collection area, high duty cycle and large aperture give Milagro unprecedented sensitivity at the highest energies (30-100 TeV). Gamma-ray radiation at these high energies is likely due to hadronic interactions since electron acceleration mechanisms are predicted to cut-off. The details of the Milagro energy spectrum analysis will be described and the energy spectrum from 5-100 TeV for all high significance detections will be presented.**

Keywords**: High-energy gamma rays**

I. Introduction

Detection of the highest energy gamma rays is critical to the understanding of the origin of galactic cosmic rays and the nature of the acceleration processes that produce them. Since cosmic-rays readily bend in Galactic magnetic fields, their trajectories can not be used to point back to their origin. Instead, accelerators can be identified by the gamma rays produced through the interaction of cosmic rays with matter in the vicinity of the accelerators. While many Galactic gamma-ray sources have been discovered at the TeV scale, identification of these source as sites of cosmic ray acceleration remains difficult since the gamma rays could also originate from electron primaries and not hadrons. The easiest way to distinguish between leptonic and hadronic origin would be the detection of neutrinos, but existing neutrino detectors lack the sensitivity to detect Galactic sources. However, at energies greater than about 50 TeV, electrons will rapidly lose energy due to synchrotron radiation in the the confining field of the accelerator. Due to their higher mass, hadrons are not subject to such a cutoff. As a consequence, spectra from Galactic gamma-ray sources that extend without a cutoff to the highest energies can be unambiguously identified to be of hadronic origin.

The experimental challenge of detecting the highest energy gamma rays is enormous. The low flux of these sources requires a detector with large collection area and long exposure times. Additionally, backgrounds from high energy cosmic rays need to be suppressed to extract the faint gamma-ray signals. The Milagro gamma-ray observatory is an air shower array that detects particles from atmospheric showers through the Cherenkov light produced in a large instrumented reservoir. Milagro continuously observes the entire overhead sky and was operated with $\sim$90% ontime for 7 years from 2000 to 2008. Unlike scintillator arrays, the water Cherenkov technique gives Milagro the ability to distinguish gamma-ray and hadron induced events with an efficiency that increases with energy.

Fig. 1. Aerial view of the Milagro detector.

II. Milagro Detector

The Milagro Detector is an air-shower array that employs a man-made pond of water instrumented with photo-multiplier tubes (PMTs) to detect Čerenkov radiation from secondary shower particles in extensive air showers. The detector is located in the Jemez mountains near Los Alamos, New Mexico at an altitude of 2650m (750g/cm^2 of overburden). The detector consists of a rectangular reservoir measuring 80m x 60m and 7m deep instrumented with 2 layers of 8" PMTs. The top layer contains 450 PMTs distributed in an 25 x 18 grid at a depth of 1.4m and is used primarily for measurement of the arrival times of secondary shower particles. The bottom layer contains 273 PMTs on a smaller 21 x 13 grid at a depth of 6m. This deep layer provides a calorimetric measurement of secondary shower particles and is used to distinguish deeply penetrating muons and hadrons, common in hadron induced air showers, from electrons and γ-rays.

The central pond detector is surrounded by an array of 175 'outrigger detectors'. The outriggers consist of

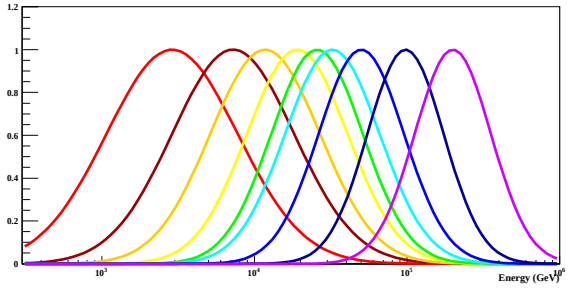

Fig. 2. Energy response and resolution of Milagro for the 9 $\mathcal{F}$ bins for source transiting at declination=22°.

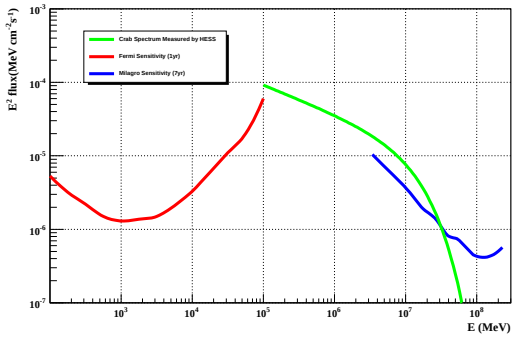

Fig. 3. The 5σ detection sensitivity of Milagro per quarter decade energy bin. Also shown are the sensitivity of Fermi [5] and the spectrum of the Crab as measured by HESS[6].

a single PMT immersed in a 4000 liter water tank. This sparse tank array covers an area of about 30,000 m^2 and is aids in angle fitting, but its primary task is locating shower cores which that fall off the central pond, which is critical for gamma-hadron separation and energy reconstruction.

The Milagro gamma-ray observatory has performed the most sensitive survey of TeV gamma rays from the northern hemisphere sky [1], [2] and detected TeV emission from a number of Galactic sources in the Fermi Bright Source List [3].

III. Energy Estimation with Milagro

When a cosmic ray or gamma ray initiates a cascade in the atmosphere the amount of energy detected at the ground depends not only on the energy of the primary particle, but also the depth of the initial interaction. Since the Milagro detector is a large area calorimeter, it is possible to measure the energy reaching the ground level with relativly small error (20-30%). However, fluctuations in the longitudinal development of atmospheric showers due primarily to fluctuations in the depth of the initial interaction will limit the energy resolution to be much worse. Gamma rays that penetrate deeply (a few radiation lengths) into the atmosphere will deliver substantially more energy at the ground level than showers that that interact at the top of the atmosphere. These fluctuations can be shown to be log-normal[4] and will dominate the energy resolution for any ground based high-energy particle detector such as Milagro.

Since the energy resolution is dominated by the characteristics of the atmosphere and not the detector's intrinsic resolution, we have designed an energy analysis for Milagro that is rather simple. We describe the energy using the parameter

$$\mathcal{F} = \frac{N_{AS}}{N_{AS}^{live}} + \frac{N_{OR}}{N_{OR}^{live}} \quad (1)$$

where $\frac{N_{AS}}{N_{AS}^{live}}$ is the fraction of live PMTs in the air shower layer which participated in the event and $\frac{N_{OR}}{N_{OR}^{live}}$ is the fraction of live outriggers that participated in the event. This parameter has a natural range from 0 to 2. We have found that more complex parameters that better estimate the energy reaching the surface only marginally increase the energy resolution. We have also considered energy parameters which include the zenith angle of the observed event, which in theory should yield better energy resolution, but in practice only marginally improve the energy resolution and substantially complicates the analysis. Furthermore, as we are analyzing data that was collected over several years of operation, the $\mathcal{F}$ parameter is ideal since it is stable through all the operational epochs.

$\mathcal{F}$	Dec=7° $(\bar{E}, \delta E)$	Dec=22°	Dec=37
0.2-0.4	3.74 0.45	3.57 0.41	3.51 0.42
0.4-0.6	4.05 0.41	3.85 0.39	3.80 0.38
0.6-0.8	4.22 0.39	4.08 0.33	4.04 0.35
0.8-1.0	4.36 0.39	4.24 0.32	4.21 0.32
1.0-1.2	4.58 0.33	4.44 0.29	4.39 0.30
1.2-1.4	4.69 0.32	4.61 0.27	4.57 0.27
1.4-1.6	4.87 0.24	4.74 0.25	4.73 0.24
1.6-1.8	5.14 0.22	4.96 0.23	4.93 0.21
1.8-2.0	5.34 0.16	5.26 0.15	5.26 0.15

TABLE I

TABLE SHOWING THE $\log_{10}$ OF THE MEDIAN ENERGY IN GEV AND ENERGY RESOLUTION FOR THE 9 $\mathcal{F}$ BINS FOR 3 SELECTED DECLINATIONS. THE ENERGY DISTRIBUTION IS GENERALLY WELL DESCRIBED AS A LOG-NORMAL DISTRIBUTION, THOUGH THAT IS NOT ASSUMED IN THIS ANALYSIS. THE ENERGY RESOLUTION IMPROVES WITH ENERGY.

IV. Data Analysis

The analysis presented here contains data from only the final 4 years of the Milagro 8 year data set. Data collected prior to the completion of the outrigger array was not included since data from the outriggers is required by the energy analysis. The Milagro data were analyzed using the method described in [2], in which the events are weighted based on the gamma/hadron separation parameter. Unlike in prior analyses, the gamma/hadron weights are optimized independently for each energy bin. This change increases the sensitivity of Milagro at the highest energies. The signal and background maps are smoothed with the point spread function, which varies based on the number energy bin. The excess (or

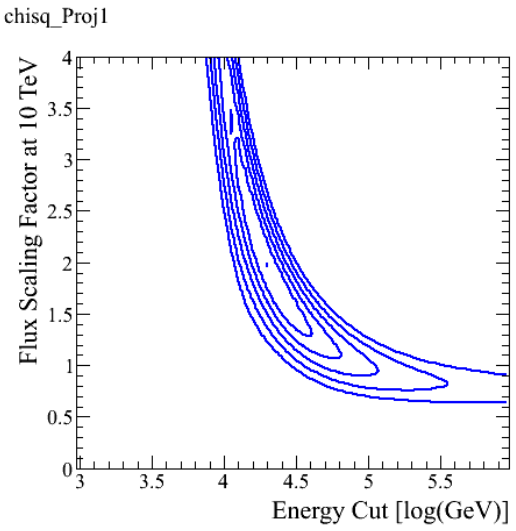

Fig. 4. 1-5 σ countours for Flux vs Cutoff Energy.

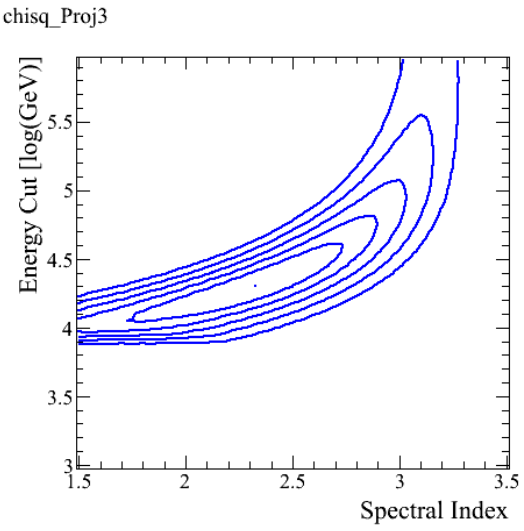

Fig. 6. 1-5 σ countours for Cutoff Energy vs Spectral Index.

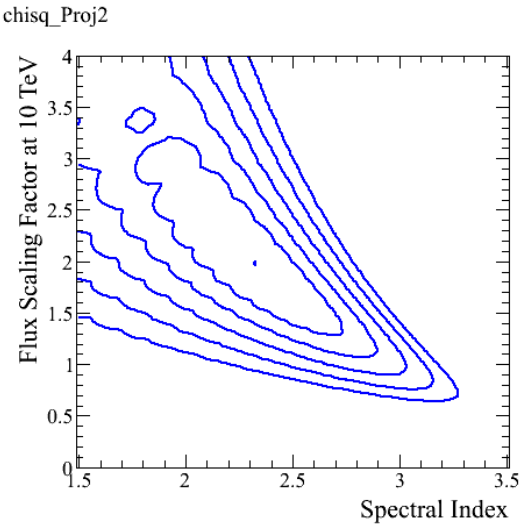

Fig. 5. 1-5 σ countours for Flux vs Spectral Index.

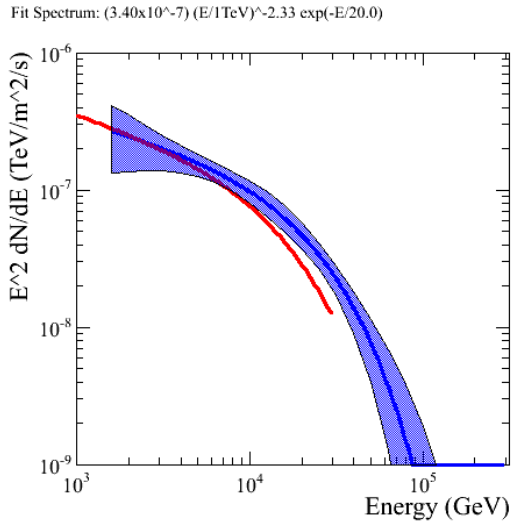

Fig. 7. 1-σ confidence interval for Milagro crab spectrum (blue) compared to the HESS crab spectrum (red).

deficit) in each $\mathcal{F}$ bin is tabulated and the statistical error is computed for each source considered.

The easiest way to proceed would be to convert the $\mathcal{F}$ excesses into fluxes, identify the typical mean energy of the events in the bin, and then fit the results to a spectral hypothesis. This approach would unfortunately not properly account for the width of the energy bins and the potentially non-Gaussian energy response of the detector. As an alternative, we perform the fit in $\mathcal{F}$ space rather than energy space. For each spectral hypothesis, we use the simulated data to predict the number of events in each $\mathcal{F}$ and compute χ^2. This approach guarantees that the energy resolution of each bin is properly considered in the fit so long as the simulation accurately describes the detector.

As a default spectral hypothesis we have chosen a power law with an exponential cut off,

$$Flux = I_0(\frac{E}{10TeV})^{-\alpha}e^{-\frac{E}{E_{cut}}}. \quad (2)$$

A 3 parameter fit is performed that minimizes χ^2 using a simple grid search algorithm.

V. Results

The results of this analysis will be presented in full at the conference. We present here only preliminary results for the spectrum of the Crab. The best fit value for the energy spectrum of the Crab is $3.4 \times 10^{-7}(\frac{E}{1TeV})^{-2.33}exp(-\frac{E}{20TeV})ph/s/m^2/TeV$. We choose not to quote the errors in the 3 fit parameters for this preliminary result, since they are highly correlated. Instead we show the contours in ChiSq space graphically. Figures 4,5 and 6 show the 1σ through

5σ contours for the 3 projections of the 3 parameter χ^2 space. These figures are not slices since for each point the displayed value of χ^2 is the minimum of the collapsed dimension. One can readily see that there is strong correlation between the fit parameters. For example, a soft spectrum hypothesis with no cutoff or a hard spectrum hypothesis with a cutoff can both adequately fit the data. This is not a phenomenon that is in any way unique to Milagro. To decouple the correlations in the fit parameters, we choose to display the spectrum as a confidence interval. Figure 7 shows the $1sigma$ confidence interval as a function of energy for the Crab spectrum. This figure is constructed by computing the range of flux values at each energy that are achievable by any combination of the 1-σ solutions. The red line in figure 7 indicates the spectrum of the crab as measured by HESS. No systematic errors are displayed.

REFERENCES

[1] Abdo, A. A., et al. 2007, ApJ Lett., **658**, L33
[2] Abdo, A. A., et al. 2007, ApJ Lett., **664**, L91
[3] arXiv:0904.1018, Submitted to Astrophysical Journal Letters.
[4] Smith, A. et al, Preceedings of the 30th ICRC (2007)
[5] See Fermi Science Support Center http://fermi.gsfc.nasa.gov/ssc/
[6] Aharonian, F. et al, Astronomy and Astrophysics, **457** 2006.